Differential Regulation of mPER1 and mTIM Proteins in the Mouse Suprachiasmatic Nuclei: New Insights into a Core Clock Mechanism

Michael H. Hastings,[1] Manuel D. Field,[1] Elizabeth S. Maywood,[1] David R. Weaver,[2] and Steven M. Reppert[2]

[1]Department of Anatomy, University of Cambridge, Cambridge CB2 3DY, United Kingdom, and [2]Laboratory of Developmental Chronobiology, Pediatric Service, Massachusetts General Hospital and Harvard Medical School, Boston Massachusetts 02214

Recent discoveries have identified a framework for the core circadian clock mechanism in mammals. Development of this framework has been based entirely on the expression patterns of so-called "clock genes" in the suprachiasmatic nuclei (SCN), the principal clock of mammals. We now provide data concerning the protein expression patterns of two of these genes, *mPer1* and *mTim*. Our studies show that mPER1 and mTIM are nuclear antigens expressed in the SCN and extensively throughout the forebrain. Expression of mPER1 in the SCN was rhythmic under entrained conditions and with clear circadian cycling under free-running conditions. Expression of mPER1 elsewhere in the mouse forebrain was not rhythmic. In contrast to mPER1, mTIM expression in the SCN did not vary with time in mice housed in either a light/dark cycle or in constant dim red light. The phase relationship between *mPer1* RNA and mPER1 cycles in the SCN is consistent with a negative feedback model of the mammalian clock. The invariant nature of nuclear mTIM in the SCN suggests that its participation in negative feedback occurs only after mPER1 has entered the nucleus, and that the abundance of mTIM is not regulated by the circadian clock or the light/dark cycle.

Key words: circadian clock; suprachiasmatic nucleus; clock gene; mPER; mTIM; negative feedback; period; timeless

Circadian timing is a fundamental property of physiology and behavior of higher organisms (Aschoff, 1981; Pittendrigh, 1993). The principal circadian clock of mammals is located in the hypothalamic suprachiasmatic nuclei (SCN) (Klein et al., 1991). The SCN clock mechanism is cell-autonomous (Welsh et al., 1995; Liu et al., 1997), possibly based on transcriptional and translational negative feedback loops (Reppert, 1998). Precedent for such a mechanism has been most fully described for circadian clocks in the fly *Drosophila melanogaster* and the fungus *Neurospora crassa* (Dunlap, 1996; Rosato et al., 1997; Young, 1998). In both organisms, autoregulatory transcriptional loops occur in which protein products of clock genes periodically enter the nucleus to suppress their own transcription. In the fly, this feedback loop involves the dynamic regulation of the clock genes *period* (*per*) and *timeless* (*tim*). As the levels of PER and TIM rise, they are phosphorylated, form heterodimers, and are then translocated to the nucleus where they shut down their own transcription. The positive factors driving *per* and *tim* transcription are dCLOCK and dBMAL1, which heterodimerize and bind to E box enhancers in the *per* and *tim* genes (Hao et al., 1997; Allada et al., 1998; Darlington et al., 1998; Rutila et al., 1998).

Mammalian homologs of *per* and *tim* have been recently cloned and characterized. A family of three mouse *(m)Per* genes has been most extensively evaluated, with each found to exhibit circadian oscillations in RNA levels in the SCN (Albrecht et al., 1997; Shearman et al., 1997; Sun et al., 1997; Tei et al., 1997; Takumi et al., 1998a,b; Zylka et al., 1998a). As in the fly, mammalian CLOCK-BMAL1 heterodimers bind E box elements in the *mPer1* gene to activate transcription (Gekakis et al., 1998). A mouse *(m)Tim* homolog has also been recently cloned and characterized (Sangoram et al., 1998; Zylka et al., 1998b). In contrast to the three *mPer* genes, however, *mTim* mRNA levels are low and nonrhythmic in the SCN. *In vitro* transcriptional studies have nonetheless shown that each of the three mPER proteins and mTIM can negatively regulate CLOCK-BMAL1-mediated transcription (Sangoram et al., 1998; Jin et al., 1999). Homodimeric and heterodimeric interactions between the three mPER proteins

Received Jan. 21, 1999; revised March 26, 1999; accepted March 30, 1999.

This work was supported by Biotechnology and Biological Sciences Research Council Project Grant 8/S07446 to M.H.H. and by National Institutes of Health Grant R37 HD14427 to S.M.R. We are extremely grateful to Jan Drew, who provided technical assistance with histology, to Dr. D. C. Hancock (Imperial Cancer Research Fund, London, UK) and I. Schurov (Department of Anatomy, University of Cambridge) for assistance with Western blot analyses, to J. O'Brien (Medical Research Council Laboratory of Molecular Biology, Cambridge, UK) for assistance with fluorescence microscopy, and to J. Bashford, A. Newman, and I. Bolton (Department of Anatomy, University of Cambridge) for assistance with photomicrography.

Correspondence should be addressed to Dr. Michael H. Hastings, Department of Anatomy, University of Cambridge, Downing Street, Cambridge CB2 3DY, UK.

Requests for reagents should be addressed to Dr. Steven M. Reppert, Laboratory of Developmental Chronobiology, Pediatric Service, GRJ 1226 Massachusetts General Hospital and Harvard Medical School, Boston, MA 02214.

This article is published in *The Journal of Neuroscience*, Rapid Communications Section, which publishes brief, peer-reviewed papers online, not in print. Rapid Communications are posted online approximately one month earlier than they would appear if printed. They are listed in the Table of Contents of the next open issue of JNeurosci. Cite this article as: JNeurosci, 1999, 0:RC11 (1–7). The publication date is the date of posting online at www.jneurosci.org.

http://www.jneurosci.org/cgi/content/full/3113

have been described that may be important for their nuclear translocation and subsequent participation in negative feedback (Zylka et al., 1998b), although the nature of physical interactions between mammalian PER and TIM and whether this contributes to nuclear translocation in the mammalian clock await clarification (Sangoram et al., 1998; Jin et al., 1999).

To understand further the roles of putative clock proteins in an SCN clock mechanism, we have generated specific antisera against mPER1 and mTIM and used them for the immunocytochemical examination of protein localization and temporal regulation in mouse forebrain and pituitary. The results of this *in vivo* analysis provide new insights into the precise roles of native mPER1 and mTIM in a core clock mechanism in the SCN. Our data also provide further evidence of dissociation between the molecular workings of mouse and fly circadian clocks.

MATERIALS AND METHODS

Antisera. Polyclonal antisera were raised in rabbits to synthetic peptides from the deduced amino acid sequence of *mPer1* and *mTim* cDNAs. The mPER1 peptide (EGADGGGDPRPGEPFC) corresponding to amino acids 6–21 (Sun et al., 1997) was synthesized at the Massachusetts General Hospital Biopolymer Core Facility. The mTIM peptide (MQNGEKSPRDPWQEDPEC) corresponding to amino acids 951–967 (Zylka et al., 1998b), plus a C-terminal C residue to permit conjugation, was synthesized at Research Genetics (Huntsville, AL). Five milligrams of each peptide were conjugated to keyhole limpet hemocyanin for immunization. Primary immunizations were performed using Freund's complete adjuvant, whereas boosts (at 2–4 week intervals) used Freund's incomplete adjuvant. Immunization protocols were conducted at Covance Research Products (Denver, PA) (mPER1) and Research Genetics (mTIM). Sera described in this report were from bleeds dated December 31, 1997 (preimmune) and June 15, 1998 from rabbit 1177 (mPER1) and July 9, 1998 (preimmune) and September 14, 1998 from rabbit 84730 (mTIM).

Animals and immunocytochemistry. All experimental manipulations were conducted under license by the Home Office, in accordance with the Animals (Scientific Procedures) Act, 1986, and the University of Cambridge code of practice for scientific procedures on animals. Adult male CD1(ICR) or C3H mice (Harlan Olac, Bicester, UK) were housed in groups of 6–10 with food and water available *ad libitum* in light-proof, ventilated chambers under a 12 hr bright white light (220 $\mu W/cm^2$), 12 hr dim red light (<5 $\mu W/cm^2$) schedule. Zeitgeber time (ZT) was defined relative to lights on (ZT0) and lights off (ZT12). To confirm entrainment and to monitor free-running activity patterns on release to constant dim red light (referred to as DD), the cages were equipped with passive infrared movement detectors linked to a computerized activity recording system (Dataquest IV; Data Sciences Inc., Frankfurt, Germany). Circadian Time (CT) was initially defined relative to predicted lights off (CT12) and on the day of sampling was confirmed by the coincident onset of group activity, as observed on the actograms. The samples for analysis of free-running cycles were taken after 12 (CT0)–34 (CT22) hr in constant dim red light. At the selected intervals, animals were killed with a barbiturate overdose and perfused through the aorta with saline followed by 4% paraformaldehyde. Brains were removed, post-fixed, transferred to cryoprotectant buffered sucrose solution (20%), and then sectioned at 40 μm on a freezing microtome. Free-floating sections were processed for immunostaining using standard procedures described previously (Ebling et al., 1991). Alternate sections were incubated with anti-mPER1 (1:8000) or anti-mTIM (1:16,000) primary sera, which were then visualized by avidin–biotin–peroxidase in conjunction with diaminobenzidine chromogen (Vector Laboratories, Peterborough, UK). Initial comparisons showed that the two strains of mice had comparable spatial and temporal patterns of expression of mPER1-ir in forebrain and pituitary; so all subsequent studies were conducted on CD1(ICR) mice. Sections were viewed on a Leitz (Wetzlar, Germany) microscope fitted with a Hamamatsu (Hamamatsu City, Japan) CCD camera (C3077) linked to an Apple (Cupertino, CA) Macintosh computer running Image version 1.49 software (a gift from Dr. W. Rashband, National Institutes of Health, Bethesda, MD) to count the number of immunoreactive nuclei above thresholded background in defined regions.

For dual immunostaining, the nuclear reaction was intensified with nickel, and sections were then processed using DAB to reveal cytoplasmic neurophysin immunoreactivity with a previously validated antiserum (Sofroniew and Weindl, 1980) generously provided by Dr. M. V. Sofroniew (Department of Anatomy, University of Cambridge). For nuclear localization of mPER1-ir, avidin-linked Cy3 fluorophore (Vector Laboratories) replaced the ABC/DAB reaction, and the sections were incubated with Hoechst stain (0.01% in PBS for 5 min) before wash and mounting. Colocalization of Hoechst-labeled nuclei and mPER1-ir was examined by switching between conventional UV fluorescence and confocal illumination on a Bio-Rad (Hercules, CA) 600 Series confocal microscope to identify mPER-ir profiles.

Western blots. Mice were killed by cervical dislocation in the middle of their light phase, their brains were rapidly removed, and the piriform cortex was microdissected. The tissue was homogenized in a Dounce homogenizer in 10 mM HEPES, 2.5 mM $MgCl_2$, 10 mM KCl with aprotinin and pepstatin at 10 μg/ml, and 5 mM dithiothreitol. Pelleted nuclei were resuspended in lysis buffer (as above with 25% glycerol and 200 μM EDTA) and respun, and the supernatant was frozen. The samples were separated on a 12 or 7.5% polyacrylamide gel, electroblotted onto a polyvinylidene difluoride membrane, and then incubated overnight with antiserum at 1:1000 dilution. Membranes were washed and processed with anti-rabbit secondary antiserum, and immunoreactive bands were visualized using ECL detection (Amersham, Buckinghamshire, UK). Specific binding was tested by preabsorbing the antiserum with the respective peptide at 10 μg/ml.

In situ *hybridization.* Mice were killed by cervical dislocation at defined daily or circadian phases, and their brains were rapidly dissected, frozen on dry ice, and stored at −45°C before sectioning on a cryostat at 16 μm. They were processed for hybridization as described previously (Simmons et al., 1989). Briefly, sections were fixed in paraformaldehyde on ice, washed with PBS, and then treated with triethanolamine and acetic anhydride and washed again. An antisense riboprobe corresponding to nucleotides 538–1752 of *mPer1* (generously provided by Professor Hitoshi Okamura, Department of Anatomy and Brain Science, Kobe University School of Medicine, Kobe, Japan) was labeled with ^{35}S-UTPαS (final activity, 1.5×10^7 cpm/ml). Sections were hybridized overnight at 58°C, washed, dehydrated as described, air-dried, and opposed to Betamax hyperfilm (Amersham) for 4 d. The relative intensity of the hybridization signal in the SCN was assessed as gray scale units above background, using the NIH Image software. A sense probe generated no specific image.

RESULTS

Characterization of mPER1- and mTIM-specific antisera

Western blots of nuclear extracts of piriform cortex probed with the mPER1 serum revealed a single band lying between 97 and 200 kDa, at a relative molecular mass of ~140 kDa, corresponding to the predicted size of native mPER1 (Fig. 1*a*). The immunostaining of the band was abrogated by preincubation of the serum with the peptide (EGADGGGDPRPGEPFC, 10 μg/ml) against which the serum was raised (Fig. 1*a*, + *lane*). A band of comparable mass was also identified by the antiserum in nuclear extracts of mouse striatum and in rat-1 fibroblast cultures, and these bands were also abrogated by preincubation with peptide (data not shown).

Immunostaining of forebrain and pituitary tissue revealed widespread expression of mPER1-ir. mPER1-ir was prominent in piriform cortex, hippocampal CA zones, pars tuberalis of the pituitary, striatum, and thalamus (data not shown). The most intense immunoreactive signal was observed in the SCN (Fig. 1*b*). Immunostaining in all of these areas, including the SCN (Fig. 1*c*), was blocked by preincubation of the primary antiserum with the peptide (10 μg/ml) used to raise it. Immunostaining was not blocked by preincubation with other peptide sequences from the mPER1 molecule (Sun et al., 1997) (amino acids 833–853, RSKAKRSRHHHHQTPRPETPC). Omission of the primary antisera also completely prevented detection of immunoreactivity, and there was no specific signal from preimmune serum.

Western blots of nuclear extracts of piriform cortex probed

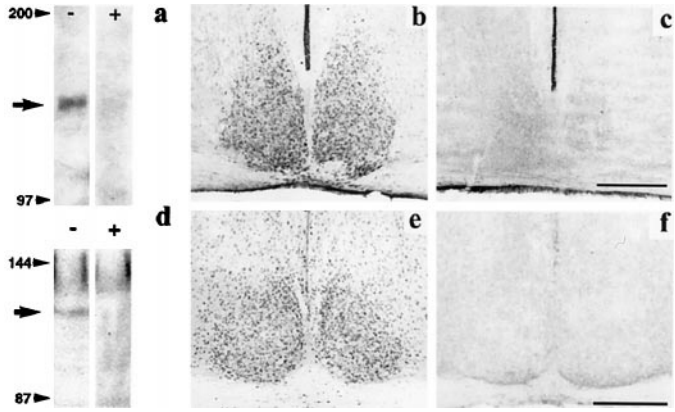

Figure 1. Characterization of mPER1 and mTIM antisera on mouse forebrain. *a*, Western blots of nuclear extracts of piriform cortex probed with anti-mPER1 serum reveal a single band (*arrow*) of ~140 kDa (− *lane*) that was blocked by preincubation with peptide (+ *lane*). Immunoreactivity to mPER1 is widespread across the forebrain, including SCN (*b*). *c*, mPER1-ir on adjacent sections was blocked by preincubation with peptide. *d*, Western blots of nuclear extracts of piriform cortex probed with anti-mTIM serum reveal a band (*arrow*) of ~120 kDa (− *lane*) that is blocked by preincubation with peptide (+ *lane*). Immunoreactivity to mTIM is widespread across the forebrain, including SCN (*e*). *f*, mTIM-ir on adjacent sections was blocked by preincubation with peptide. All images are representative of at least three independent experiments. Scale bar, 200 μm.

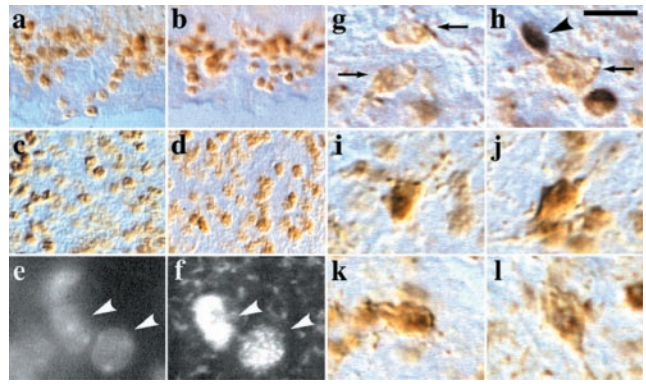

Figure 2. Nuclear localization of mPER1 and mTIM in mouse forebrain and pituitary. High-power (40×) images of pars tuberalis (*a, b*) adherent to ventral surface of hypothalamus, and ventral SCN (*c, d*), viewed under contrast interference, reveal nuclear profiles of mPER1-ir (*a, c*) and mTIM-ir (*b, d*). High-power (60×) views of SCN nuclei visualized with Hoechst stain (*e*) and fluorescent mPER1-ir (*f*) confirm nuclear localization of mPER1. Representative high-power (40×) images of dual-labeled SCN neurons viewed under contrast interference reveal *brown* immunoreaction for neurophysin and *blue–black* immunoreaction for mPER1. Tissue sampled at ZT0–2 (*g, h*) contains neurophysin-ir perikarya (*arrows*) devoid of nuclear mPER1-ir, although sporadic non-neurophysin cells with nuclear mPER1-ir profiles are evident (*arrowhead*). Tissue sampled at ZT12–16 (*i–l*) revealed neurophysin-ir perikarya with mPER1-ir nuclei. Scale bar: *a–d*, 40 μm; *e, f*, 10 μm; *g–l*, 20 μm.

with the mTIM antiserum revealed several immunoreactive bands between 87 and 144 kDa (Fig. 1*d*, − *lane*). Preincubation of the antiserum with peptide used to raise the antiserum (MQNGEKSPRDPWQEDPE, 10 μg/ml) abrogated the immunostaining of a band with a relative molecular mass of ~120 kDa (Fig. 1*d*, + *lane*), corresponding to the predicted size of native mTIM. Adjacent bands were not affected by the peptide, indicative of nonspecific staining. A band of comparable mass was also identified by the antiserum in nuclear extracts of mouse striatum, and a band of slightly lighter mass was detected in Swiss 3T3 cells. Both bands were also abrogated by preincubation of the serum with peptide (data not shown).

Immunoreactivity to mTIM was widespread throughout the mouse forebrain, including piriform cortex and hippocampal CA zones, and the SCN. By far the most intense immunoreactivity was observed in the pars tuberalis of the pituitary, an area reported to contain high levels of *mTim* mRNA (Zylka et al., 1998b). Immunoreaction in the SCN and elsewhere was modest (Fig. 1*e*), but in all cases it was specific, being blocked by preincubation with the peptide (Fig. 1*f*). Immunoreactivity was also lost on omission of the primary antisera, and the preimmune serum did not generate any specific signal (data not shown).

Nuclear localization of mPER1-ir and mTIM-ir

Under high power (40 and 60×) and viewed with contrast interference optics, the mPER1-ir and mTIM-ir profiles in the pars tuberalis (Fig. 2*a,b*) and SCN (Fig. 2*c,d*) were clearly nuclear. There was no indication of cytoplasmic mPER1-ir or mTIM-ir in any tissues examined. Further confirmation of the nuclear localization of mPER1-ir was provided by colabeling with Hoechst stain, which identified all nuclei in the SCN (Fig. 2*e*), a number of which were immunopositive for mPER1-ir (Fig. 2*f*). The profile of mPER1-ir did extend beyond the nucleus, as defined by the Hoechst stain.

Expression of mPER1-ir in the SCN exhibits daily and circadian cycles

The distribution and abundance of mPER1-ir in the SCN changed dramatically across the 24 hr period in mice housed in a light/dark (LD) cycle. During the early light phase, there were relatively few mPER1-ir nuclei in the SCN (Fig. 3*a*). Sporadic immunoreactive nuclei were evident in the dorsolateral region. Immunoreactivity became more extensive over the course of the day, and by the end of the light phase (ZT12; Fig. 3*b*) many cells in all areas of the SCN appeared to be expressing high levels of nuclear mPER1-ir. This level of expression persisted into the early dark phase, but beyond ZT18 there was a progressive decline in the expression of mPER1-ir.

This daily variation in mPER1-ir was confirmed by cell counts, which revealed a highly significant effect of time on the number of mPER1-ir nuclei in the SCN (Fig. 3*c*). Levels rose rapidly between ZT4 and ZT8, remained significantly elevated above ZT0 counts from ZT8 until ZT18, and then fell rapidly to a minimum by ZT22.

The daily cycle of mPER1-ir was specific to the SCN. No other forebrain regions exhibited any systematic change over the 24 hr interval (data not shown). Although nuclear mPER1-ir was evident in the pars tuberalis at all phases of the circadian cycle, no systematic variation in cell number or intensity of reaction product could be identified.

In a parallel group of animals, *mPer1* mRNA expression was examined by *in situ* hybridization. Across the forebrain of CD1 mice, the pattern of hybridization was consistent with that reported previously for C57Bl/6 (Shearman et al., 1997), BALB/c (Tei et al., 1997), and CD1 Sangoram et al. (1998) mice, with high expression in piriform cortex, neocortex, thalamus, striatum, and hippocampus. The most intense signal was evident in the SCN, dependent on phase. *mPer1* hybridization signal in the SCN was maximal at ZT6, remained high until ZT12, and then fell precipitously to its minimum in the late dark phase (Fig. 3*c*). The

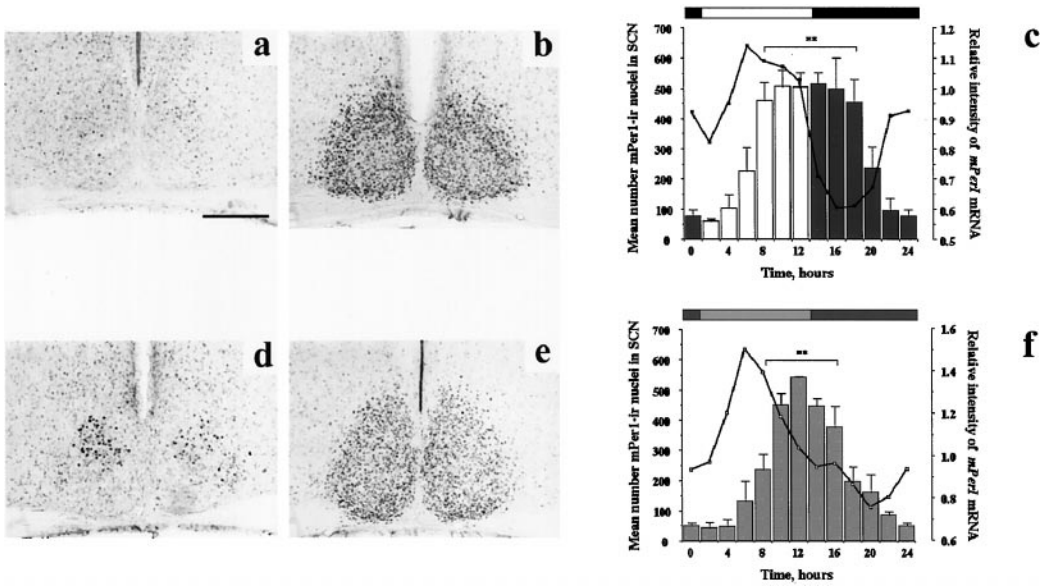

Figure 3. Nuclear mPER1 in mouse SCN shows daily and circadian cyclicity. Representative photomicrographs of coronal sections of SCN of mice entrained to 12 hr LD reveal low levels of mPER1 expression at the end of the dark phase, ZT0 (*a*), but extensive nuclear mPER1-ir at the end of the light phase, ZT12 (*b*). *c*, In mice entrained to 12 hr LD, the mean number of mPER1-ir nuclei in the SCN increases during the light phase and falls in the late dark phase, exhibiting a significant daily rhythm (ANOVA time effect, $F = 10.4$; $p < 0.01$), which is phase-delayed relative to the mRNA cycle by 4–6 hr. *d*, In mice free-running in continuous dim red light, mPER1-ir was low at CT0, with a limited number of dorsolateral cells, but by CT12 (*e*), levels were maximal, with immunoreactive nuclei throughout the SCN. *f*, In mice free-running in continuous dim red light, the mPER1 rhythm peaks at CT12 (ANOVA time effect, $F = 17.5$; $p < 0.01$) and is phase-delayed relative to the mRNA peak by ~6 hr. mPER1 data are plotted as mean +SEM from three independent experiments. Two-way ANOVA revealed a highly significant overall effect of time ($F = 24.2$; $p < 0.01$) and also a significant difference between lighting conditions ($F = 14.3$; $p < 0.01$), with levels being significantly higher overall in the mice exposed to light, reflecting the prolonged peak of mPER1 expression. $^{**}p < 0.01$ versus ZT0 or CT0, respectively, by Dunnett's *t* test. The relative intensity of hybridization signal for *mper1* mRNA was determined from single animals at each time point and is presented as a two-point moving average. Data for ZT0 and CT0 replotted as ZT24 and CT24 for clarity.

cycles of *mPer1* mRNA and protein were clearly in different phases, the rise in protein levels occurring after the increase in mRNA abundance with a lag of ~4–6 hr. The subsequent decline in mRNA was coincident with the sustained abundance of nuclear protein levels, and mRNA abundance did not increase until protein levels started to fall at the end of the night.

The variation in mPER1-ir in the SCN was maintained in animals exposed to continuous dim red light, confirming its circadian nature (Fig. 3*d,e*). Levels of mPER1-ir were low at CT0, although the dorsolateral population of mPER1-ir nuclei was very apparent at CT0. The number of immunoreactive nuclei was significantly elevated from CT8 to CT16, falling to a minimum by CT22 (Fig. 3*f*).

Statistical comparison of the temporal patterns of mPER1-ir between mice in LD and those in DD revealed that the protein cycle was significantly different ($p < 0.01$) between entrained and free-running conditions. Although peak levels of abundance were not different, the peak in expression was more transient in DD than in animals exposed to LD. This difference in the pattern of mPER1-ir was also reflected in the patterns of mRNA expression, in that the duration of elevated *mPer1* expression appeared to be greater in LD than DD (Fig. 3*c,f*), although statistical comparison was not possible with the limited sample size. In both lighting conditions, the peak in the mRNA cycle preceded the peak in the protein cycle by 4–6 hr. In DD, the decline in mRNA abundance was coincident with the increase in nuclear mPER1-ir, whereas in LD the levels of *mPer1* mRNA remained elevated even after nuclear mPER1 reached peak levels.

To examine the nuclear localization of mPER1 in a temporal context, it was combined with immunostaining for neurophysin, a cytoplasmic protein of vasopressinergic neurons in the SCN. As anticipated, the neurophysin antiserum identified perikarya (Fig. 2*g,h*) in the dorsal and medial divisions of the SCN, plus a discrete laterally placed group. When sampled during ZT0–2 and CT0–2, the nuclei of neurophysin-ir neurons were devoid of mPER1-ir, although a few mPER1-ir nuclei could be identified adjacent to the neurophysin perikarya. In contrast, in animals sampled between ZT10–16 and CT10–12, a number of neurophysin-ir profiles could be seen to contain mPER1-ir nuclei (Fig. 2*i–l*), confirming mPER1 as a nuclear antigen. Of 658 vasopressinergic perikarya examined from four mice at ZT0–2, none exhibited nuclear mPER1-ir. In contrast, at the peak of expression of mPER1-ir at ZT12–16, most vasopressinergic neurons [220 of 336 (66%) from 10 mice] had nuclear mPER1-ir. This rhythmic expression of nuclear mPER1-ir in vasopressinergic cells was specific to the SCN. At no stage was mPER1-ir observed in the magnocellular vasopressinergic cells of the supraoptic and paraventricular nuclei (data not shown).

Expression of mTIM-ir in the SCN is constitutive

The distribution of mTIM-ir in the SCN corresponded very closely to that observed for mPER1 on adjacent sections from the same brains sampled at ZT12. In all cases mTIM-ir was nuclear in localization. However, in marked contrast to mPER1-ir, the distribution and abundance of mTIM-ir in the SCN did not vary significantly with Zeitgeber (Fig. 4*a–c*) or circadian time (Fig. 4*d–f*), nor was there a difference between the two lighting conditions. It is worth noting that there were clear daily and circadian changes in mPER1-ir on adjacent sections from the same animals that showed no change in mTIM-ir. The number of mTIM-ir

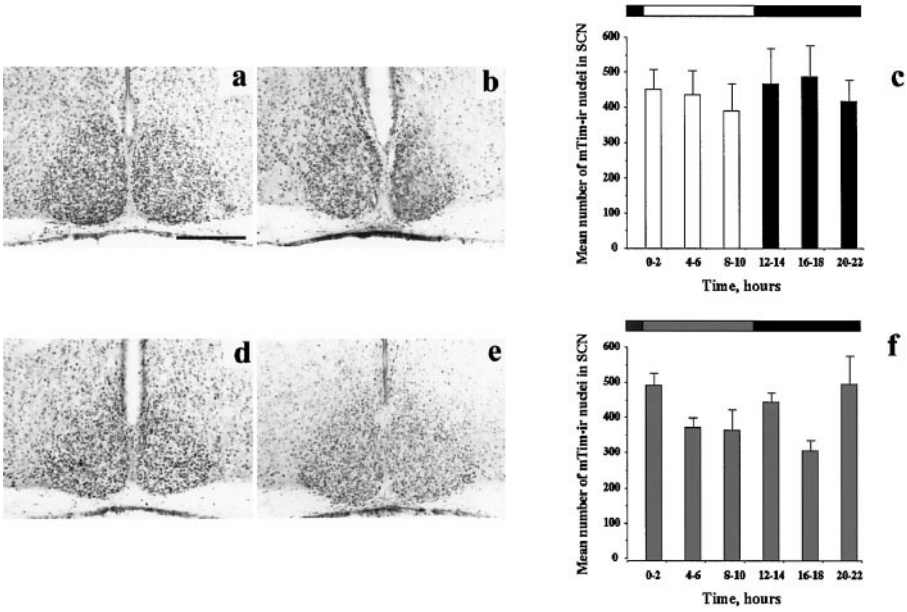

Figure 4. Nuclear mTIM-ir in the mouse SCN does not show any daily or circadian variation. *a* In mice sampled at the beginning of the light phase (ZT0), representative coronal sections demonstrate that mTIM-ir nuclei are abundant throughout the SCN and adjacent hypothalamus. A similar pattern of expression is observed at the end of the light phase (ZT12) (*b*), and cell counts (mean + SEM; $n = 6$ per group) reveal no systematic change in abundance of mTIM over the day (*open bars*) and night (*shaded bars*) (*c*). *d*, In mice free-running under continuous dim red light and sampled at CT0, mTIM-ir nuclei were extensive across the whole SCN and adjacent hypothalamus, and the expression pattern at CT12 (*e*) was comparable with that at CT0 and ZT12. *f*, The abundance of mTIM-ir nuclei in the SCN was continuously high under free-running conditions in the absence of light (*shaded bars*). Two-way ANOVA revealed no difference over time (time effect, $F = 1.52$; NS) or between lighting conditions (treatment effect, $F = 0.44$; NS) and no interaction ($F = 1.37$; NS).

nuclei in the SCN, ~450–500 per 40 μm section, was directly comparable with the peak number of mPER1-ir cells in the SCN under both entrained and free-running conditions. The intensity of mTIM-ir in the SCN was lower than the intensity of mPER1-ir at peak phases, however, and was also lower than the intensity of mTIM-ir in the pars tuberalis from the same animals. The high level of mTIM expression in the pars tuberalis was maintained under both lighting regimens and did not show any systematic variation (data not shown). Unvarying expression of nuclear mTIM-ir was also noted in other forebrain regions, including piriform cortex and hippocampus.

DISCUSSION

The distribution of mPER1-ir in forebrain and pars tuberalis of the pituitary corresponded closely with *mPer1* expression assessed by *in situ* hybridization in CD1 (present study) and C57Bl/6 mice (Shearman et al., 1997). Modest expression of mTIM-ir in the forebrain of CD1 mice and much higher levels in the pars tuberalis are also consistent with patterns of gene expression in C57Bl/6 and CD1 mice (Sangoram et al., 1998; Zylka et al., 1998b). In all areas and times examined, immunoreactivity was localized to the nucleus: there was no evidence for cytoplasmic expression of either antigen. In most regions of the forebrain, expression of both proteins is constitutive. In the SCN, however, mPER1-ir is robustly rhythmic in LD, peaking in the later light phase and early dark phase. Moreover, the rhythm in mPER1-ir is circadian, persisting in animals exposed to DD. The *mPer1* RNA cycle precedes the mPER1 protein cycle by 4–6 hr in both LD and DD, consistent with a role for the mPER protein in the autoregulation of its transcription. mTIM expression, on the other hand, is invariant in the SCN; it is regulated by neither the light dark cycle nor the circadian cycle. Although the nuclear localization of mPER1 and mTIM suggests that each is involved in regulating transcriptional processes, our data provide further evidence that TIM function in a core clock mechanism differs between mammals and *Drosophila*.

The phase relationship of the *mPer1* RNA (Sun et al., 1997; Tei et al., 1997; Shearman et al., 1998) and protein cycles in the SCN is strikingly similar to that observed for both *per* and *tim* RNA and protein cycles in *Drosophila* (Rosato et al., 1997; Young, 1998). The peak of nuclear mPER1-ir in animals held on LD coincides with the decline in *mPer1* mRNA levels. This behavior of the native protein is consistent with its proposed negative feedback role (Reppert, 1998) and the reported actions of the recombinant protein *in vitro* (Sangoram et al., 1998; Jin et al., 1999). As high protein levels begin to decline, negative feedback is presumably relieved, and the *mPer1* mRNA level rises. This pattern persists in DD, but the duration of the protein peak (and possibly the RNA peak) is truncated compared with that in LD, which may reflect a direct effect of light in activating *mPer1* expression, with a concomitant increase in the duration of mPER1 expression.

In the feedback loop model of the fly clock, delays in various stages of the cycle establish and maintain its spontaneous oscillation and 24 hr period. dPER is progressively phosphorylated, which destabilizes monomeric protein so that PER accumulation and heterodimerization with TIM only occur when TIM levels are rising (Kloss et al., 1998; Price et al., 1998). PER-TIM heterodimers in turn are an apparent necessary precursor to translocation to the nucleus (Saez and Young, 1996). The current results suggest that the mammalian clock loop involves similar delays between *mPer1* mRNA and protein. Destabilization of the mPER1 protein by phosphorylation could explain the lack of detection of a cytoplasmic phase of mPER1 in the SCN, although it cannot be excluded that mPER1 is present in the cytoplasm but in a form not recognized by the antiserum. However, it is unlikely that the lack of detection of cytoplasmic mPER1 reflects the constitutive availability of mTIM as a potential partner to mPER1, immediately shuttling newly synthesized protein into the nucleus. If this were the case, there should be a substantial change in the intensity of nuclear mTIM staining in the SCN as mPER1 begins to flood the nucleus. There was no evidence, however, of a daily oscillation in the intensity of mTIM staining in the nuclei of SCN cells or any evidence of cytoplasmic accumulation of mTIM at any time of day. Furthermore, mTIM is nuclear even in areas in which mPER1 is not expressed (SCN during early subjective day, peri-SCN hypothalamus and habenular nuclei at all phases), suggesting that nuclear targeting of mTIM does not require interaction with mPER1.

Although it cannot be excluded that a small, undetectable fraction of the available mTIM acts as a shuttling partner, the most likely partners for nuclear translocation of mPER1 are the other mPER proteins. Extensive pairwise associations among the three mPER proteins (but not mPER and mTIM) have been reported using yeast two-hybrid assays, suggesting that mPER1 associates with mPER2 and/or mPER3 to enter the nucleus of SCN neurons (Zylka et al., 1998b). The expression of the *mPer2* and *mPer3* genes lags slightly behind that of *mPer1* (Takumi et al., 1998a,b; Zylka et al., 1998a); so a delayed availability of mPER2 and mPER3 partners may contribute to the delay between the peaks of *mPer1* mRNA and nuclear mPER1. In other forebrain regions the constitutive nuclear expression of mPER1 suggests that there is no circadian or daily gate to nuclear translocation, consistent with nonrhythmic and constitutive expression of the other *mPer* genes in these tissues (Takumi et al., 1998a,b; Zylka et al., 1998a).

Despite the dramatic changes in mPER1 distribution and intensity in the SCN, protein expression was constantly maintained in a small population of cells in a characteristic dorsolateral position, overlapping the distribution of arginine vasopressin (AVP) neurons. However, the mPER1-ir cells were not neurophysin-ir, and AVP cells, in common with the bulk of SCN neurons, exhibit a cycle of mPER1 expression, consistent with the recent demonstration of the ability of mPER proteins to control rhythmic transcription of the AVP gene via a negative regulation of CLOCK-BMAL1 activation (Jin et al., 1999). The peak of AVP transcription in the SCN is during subjective day (Carter and Murphy, 1992). The increase in abundance of mPER1 protein in AVP neurons during late subjective day and subsequent decline in late subjective night are therefore likely to be a major contributor to the AVP transcriptional rhythm and consequent circadian pattern of AVP (Reppert et al., 1987). The mPER1 data provided in this paper thus contribute to the recent finding that the transcriptional machinery of the core clockwork can directly regulate clock-controlled output rhythms (Jin et al., 1999).

The spatial and temporal patterns of expression of mTIM in the forebrain and pars tuberalis extend recent reports describing the distribution and temporal pattern of *mTim* RNA levels. *mTim* gene expression is higher in the pars tuberalis than the brain, and its levels of expression in the SCN are moderate and do not change appreciably with daily or circadian stage (Sangoram et al., 1998; Zylka et al., 1998b). This contrasts markedly with the behavior of dTIM, which plays a number of key roles in the *Drosophila* core oscillation (Rosato et al., 1997; Young, 1998).

First, *dtim* is rhythmically expressed at the level of mRNA and protein and thereby contributes to the circadian gate for nuclear entry of dPER (Saez and Young, 1996). The invariant nature of nuclear mTIM in the SCN suggests that it is not involved in the circadian gating of the nuclear translocation of mPER1. It is entirely possible, however, that mTIM is an important nuclear cofactor for negative regulation of CLOCK-BMAL1-mediated transcription. For example, mTIM may complex with mCLOCK once it has translocated to the nucleus. This would fit with the ability of mTIM to shut down CLOCK-BMAL1-mediated transcription *in vitro* (Sangoram et al., 1998; Zylka et al., 1998b). It is also consistent with the notion based on studies in *Drosophila* that dPER-dTIM-dCLOCK complexes shut down *per* and *tim* transcription (Lee et al., 1998). We thus propose that mTIM is a nuclear cofactor important for negative regulation of CLOCK-BMAL1-mediated transcription once mPER1 has entered the nucleus but that mTIM is not necessary for the translocation of mPER1 from cytoplasm to nucleus. Such a scenario would represent a clear evolutionary dissociation between the effects of TIM on the negative limb of the fly and mouse circadian feedback loop.

A second difference between mTIM and dTIM is light regulation. In the fly, dTIM is rapidly degraded by exposure to light and thereby provides a mechanism for photic resetting of the oscillator (Hunter-Ensor et al., 1996; Myers et al., 1996). There was no evidence, however, of photic sensitivity of mTIM in the current study. Moreover, exposure to nocturnal light pulses has no detectable effect on mTIM levels in the SCN (our unpublished data). Comparison of light regulation of the core oscillator of the mouse and fly therefore reveals a second evolutionary dissociation, with photic regulation involving degradation of dTIM in the fly but induction of *mPer1* and *mPer2* in the mouse (Albrecht et al., 1997; Shearman et al., 1997; Shigeyoshi et al., 1998).

A general framework for a central clock mechanism in mammals is now in place. Even at this early stage, significant differences in the molecular details of a clock feedback loop exist between the mouse and the fly and between the fly and the silk moth (Sauman and Reppert, 1996). Continued comparisons of molecular mechanisms in a wide array of animals will add to our understanding of the various ways in which common elements can interact to yield a core clock mechanism.

REFERENCES

Albrecht U, Sun ZS, Eichele G, Lee CC (1997) A differential response of two putative mammalian circadian regulators, *mper1* and *mper2*, to light. Cell 91:1055–1064.

Allada R, White NE, So WV, Hall JC (1998) A mutant *Drosophila* homolog of mammalian *Clock* disrupts circadian rhythms and transcription of *period* and *timeless*. Cell 93:791–804.

Aschoff J (1981) Handbook of behavioral neurobiology, Vol 4, Biological rhythms. New York: Plenum.

Carter DA, Murphy D (1992) Nuclear mechanisms mediate rhythmic changes in vasopressin mRNA expression in the rat suprachiasmatic nucleus. Mol Brain Res 12:315–321.

Darlington TK, Wager-Smith K, Ceriani MF, Staknis D, Gekakis N, Steeves TDL, Weitz CJ, Takahashi JS, Kay SA (1998) Closing the circadian loop: CLOCK-induced transcription of its own inhibitors, *per* and *tim*. Science 280:1599–1603.

Dunlap JC (1996) Genetics and molecular analysis of circadian rhythms. Annu Rev Genet 30:579–601.

Ebling FJP, Maywood ES, Staley K, Humby T, Hancock DC, Waters CM, Evan GI, Hastings MH (1991) The role of NMDA-type glutamatergic neurotransmission in the photic induction of immediate-early gene expression in the suprachiasmatic nuclei of the Syrian hamster. J Neuroendocrinol 3:641–652.

Gekakis N, Staknis D, Nguyen HB, Davis FC, Wilsbacher LD, King DP, Takahashi JS, Weitz CJ (1998) Role of the CLOCK protein in the mammalian circadian mechanism. Science 280:1564–1569.

Hao H, Allen DL, Hardin PE (1997) A circadian enhancer mediates PER-dependent mRNA cycling in *Drosophila melanogaster*. Mol Cell Biol 17:3687–3693.

Hunter-Ensor M, Ousley A, Seghal A (1996) Regulation of the *Drosophila* protein Timeless suggests a mechanism for resetting the circadian clock by light. Cell 84:677–685.

Jin X, Shearman LP, Weaver DR, Zylka MJ, de Vries GJ, Reppert SM (1999) A molecular mechanism regulating rhythmic output from the suprachiasmatic circadian clock. Cell 96:57–68.

Klein DC, Moore RY, Reppert SM (1991) Suprachiasmatic nucleus: the mind's clock. New York: Oxford UP.

Kloss B, Price JL, Saez L, Blau J, Ruthenfluh A, Wesley CS, Young MW (1998) The *Drosophila* clock gene *double-time* encodes a protein closely related to human casein kinase IE. Cell 94:97–107.

Lee C, Bae K, Edery I (1998) The *Drosophila* CLOCK protein undergoes daily rhythms in abundance, phosphorylation, and interactions with the PER-TIM complex. Neuron 21:857–867.

Liu C, Weaver DR, Strogatz SH, Reppert SM (1997) Cellular construction of a circadian clock: period determination in the suprachiasmatic nuclei. Cell 91:855–860.

Myers MP, Wager-Smith K, Rothenfluh-Hifiker A, Young MW (1996) Light-induced degradation of TIMELESS and entrainment of the *Drosophila* circadian clock. Science 271:151–152.

Pittendrigh CS (1993) Temporal organization: reflections of a Darwinian clock-watcher. Annu Rev Physiol 55:16–54.

Price JL, Blau J, Ruthenfluh A, Aboodeely M, Kloss B, Young MW (1998) Double-time is a new *Drosophila* clock gene that regulates PERIOD protein accumulation. Cell 94:83–95.

Reppert SM (1998) A clockwork explosion! Neuron 21:1–4.

Reppert SM, Schwartz WJ, Uhl GR (1987) Arginine vasopressin: a novel peptide rhythm in cerebrospinal fluid. Trends Neurosci 10:76–80.

Rosato E, Piccin A, Kyriacou CP (1997) Molecular analysis of circadian behaviour. Bioessays 19:1075–1082.

Rutila JE, Suri V, Le M, So MV, Rosbash M, Hall JC (1998) CYCLE is a second bHLH-PAS clock protein essential for circadian rhythmicity and transcription of *Drosophila period* and *timeless*. Cell 93:805–814.

Saez L, Young MW (1996) Regulation of nuclear entry of the *Drosophila* clock proteins Period and Timeless. Neuron 17:911–920.

Sangoram AM, Saez L, Antoch MP, Gekakis N, Staknis D, Whiteley N, Fruechte EM, Vitaterna MH, Shimomura K, King DP, Young MW, Weitz CJ, Takahashi JS (1998) Mammalian circadian autoregulatory loop: a *Timeless* ortholog and *mPer1* interact and negatively regulate CLOCK-BMAL1-induced transcription. Neuron 21:1101–1113.

Sauman I, Reppert SM (1996) Circadian clock neurons in the silkmoth *Antheraea pernyi*: novel mechanisms of period protein regulation. Neuron 17:889–900.

Shearman LP, Zylka MJ, Weaver DR, Kolakowski Jr LF, Reppert SM (1997) Two *period* homologs: circadian expression and photic regulation in the suprachiasmatic nuclei. Neuron 19:1261–1269.

Shigeyoshi Y, Taguchi K, Yamamoto S, Takekida S, Yan L, Tei H, Moriya T, Shibata S, Loros JJ, Dunlap JC, Okamura H (1998) Light-induced resetting of a mammalian circadian clock is associated with rapid induction of the *mPer1* transcript. Cell 91:1043–1053.

Simmons DM, Arriza JL, Swanson LW (1989) A complete protocol for *in situ* hybridization of messenger RNAs in brain and other tissues with radiolabelled single-stranded RNA probes. J Histotechnol 12:169–181.

Sofroniew MV, Weindl A (1980) Identification of parvocellular vasopressin and neurophysin neurons in the suprachiasmatic nucleus of a variety of mammals including primates. J Comp Neurol 193:659–675.

Sun ZS, Albrecht U, Zhuchenko O, Bailey J, Eichele G, Lee CC (1997) RIGUI, a putative mammalian ortholog of the *Drosophila period* gene. Cell 90:1003–1011.

Takumi T, Matsubara C, Shigeyoshi Y, Taguchi K, Yagita K, Maebayashi Y, Sakakida Y, Okamura K, Takashima N, Okamura H (1998a) A new mammalian period gene predominantly expressed in the suprachiasmatic nucleus. Genes Cells 3:167–176.

Takumi T, Taguchi K, Miyake S, Sakakida Y, Takashima N, Matsubara C, Maebayashi Y, Okamura K, Takakida S, Yamamoto S, Yagita K, Yan L, Young MW, Okamura H (1998b) A light-independent oscillatory gene *mPer3* in mouse SCN and OVLT. EMBO J 17:4753–4759.

Tei H, Okamura H, Shigeyoshi Y, Fukuhara C, Ozawa R, Hirose M, Sakaki Y (1997) Circadian oscillation of a mammalian homologue of the *Drosophila period* gene. Nature 389:512–516.

Welsh DK, Logothetis DE, Meister M, Reppert SM (1995) Individual neurons dissociated from rat suprachiasmatic nucleus express independently phased circadian firing rhythms. Neuron 14:697–706.

Young MW (1998) The molecular control of circadian behavioral rhythms and their entrainment in *Drosophila*. Annu Rev Biochem 67:135–152.

Zylka MJ, Shearman LP, Weaver DR, Reppert SM (1998a) Three *period* homologs in mammals: differential light responses in the suprachiasmatic circadian clock and oscillating transcripts outside of brain. Neuron 20:1103–1110.

Zylka MJ, Shearman LP, Levine JD, Jin X, Weaver DR, Reppert SM (1998b) Molecular analysis of mammalian *Timeless*. Neuron 21: 1115–1122.